Journal of Clinical and Translational Hepatology **2022** vol. 10(3) | 429–438
DOI: 10.14218/JCTH.2021.00108

Original Article

Dermcidin Enhances the Migration, Invasion, and Metastasis of Hepatocellular Carcinoma Cells *In Vitro* and *In Vivo*

Fanghua Qiu[1], Huajing Long[2], Lu Zhang[2], Jieyuan Liu[3], Zetian Yang[2] and Xianzhang Huang[4*]

[1]Department of Hospital Acquired Infection Control, Affiliated TCM Hospital of Guangzhou Medical University, Guangzhou, China; [2]Guangzhou University of Chinese Medicine, Guangzhou, China; [3]University of California, San Diego, Warren College, San Diego, CA, USA; [4]Department of Clinical Laboratory, Second Affiliated Hospital, Guangzhou University of Chinese Medicine, Guangzhou, China

Received: 24 March 2021 | **Revised:** 9 July 2021 | **Accepted:** 17 September 2021 | **Published:** 4 January 2022

Abstract

Background and Aims: Hepatocellular carcinoma (HCC) is a common primary liver neoplasm with high mortality. Dermcidin (DCD), an antimicrobial peptide, has been reported to participate in oncogenesis. This study assessed the effects and underlying molecular events of DCD overexpression and knockdown on the regulation of HCC progression *in vitro* and *in vivo*. ***Methods:*** The serum DCD level was detected using enzyme-linked immunosorbent assay. DCD overexpression, knockdown, and Ras-related C3 botulinum toxin substrate 1 (Rac1) rescue were performed in SK-HEP-1 cells using plasmids. Immunofluorescence staining, quantitative PCR, and Western blotting were used to detect the expression of different genes and proteins. Differences in HCC cell migration and invasion were detected by Transwell migration and invasion assays. A nude mouse HCC cell orthotopic model was employed to verify the *in vitro* data. ***Results:*** The level of serum DCD was higher in patients with HCC and in SK-HEP-1 cells. DCD overexpression caused upregulation of *DCD*, *fibronectin*, *Rac1*, and cell division control protein 42 homologue (*Cdc42*) mRNA and proteins as well as actin-related protein 2/3 (Arp2/3) protein (but reduced *Arp2/3* mRNA levels) and activated Rac1 and Cdc42. Phenotypically, DCD overexpression induced HCC cell migration and invasion *in vitro*, whereas knockout of DCD expression had the opposite effects. A Rac1 rescue experiment in DCD-knockdown HCC cells increased HCC cell migration and invasion and increased the levels of active Rac1/total Rac1, Wiskott-Aldrich syndrome family protein (WASP), Arp2/3, and fibronectin. DCD overexpression induced HCC cell metastasis to the abdomen and liver *in vivo*. ***Conclusions:*** DCD promotes HCC cell migration, invasion, and metastasis through upregulation of noncatalytic region of tyrosine kinase adaptor protein 1 (Nck1), Rac1, Cdc42, WASP, and Arp2/3, which induce actin cytoskeletal remodeling and fibronectin-mediated cell adhesion in HCC cells.

Citation of this article: Qiu F, Long H, Zhang L, Liu J, Yang Z, Huang X. Dermcidin Enhances the Migration, Invasion, and Metastasis of Hepatocellular Carcinoma Cells *In Vitro* and *In Vivo*. J Clin Transl Hepatol 2022;10(3):429–438. doi: 10.14218/JCTH.2021.00108.

Introduction

Hepatocellular carcinoma (HCC) is a common primary liver neoplasm with high mortality, and it imposes a significant health and economic burden worldwide.[1] HCC risk factors include hepatitis virus B and/or C infection and alcohol consumption leading to the dysregulation of cell signaling transduction pathways, such as MAPK, AKT and ERK, imbalance between the activities of proto-oncogenes and tumor suppressor genes, and immortal proliferation of liver cancer stem cells.[2–4] High HCC mortality and poor prognosis are mainly due to tumor metastasis, and the underlying molecular mechanism of HCC metastasis has been extensively studied. Many genes participate in the process of HCC metastasis, including *EGFR*, *TP53*, *APP*, *VEGFA*, *MAPK1*, *PI3KCA*, and *MMP9*.[5] However, further investigation of the genes and gene pathways in HCC metastasis could help us control HCC more effectively in the future.

Dermcidin (DCD) was originally identified in eccrine sweat glands. With a molecular weight of 11.2 kDa, as a precursor protein, DCD is composed of 110 amino acid residues.[6,7] After the removal of the first 19-amino acid signal peptide, the precursor matures to a secreted protein with a 9.5 kDa molecular weight. In eccrine sweat, DCD is further proteolytically processed into many active peptides with different antimicrobial activities.[6–9] Moreover, DCD is putatively produced and processed by cancer cells, including those of melanoma,[10] pancreatic cancer,[11,12] breast cancer,[11,13,14] gastroesophageal tumors,[15] leukemia,[16,17] and HCC.[18] DCD participates in oncogenesis[19] and induces cancer cachexia and cancer cell growth and survival[20] but reduces serum dependency[19] for tumor invasion[21] and migration.[22] Thus, DCD expression may contribute to cancer progression and a

Keywords: Hepatocellular carcinoma; Dermcidin; Metastasis; Gene regulation; Cell adhesion.

Abbreviations: Arp2/3, actin-related protein 2/3; AUC, area under the ROC curve; Cdc42, cell division control protein 42 homologue; CI, confidence interval; DCD, dermcidin; ELISA, enzyme-linked immunosorbent assay; HCC, hepatocellular carcinoma; NC, negative control; Nck1, noncatalytic region of tyrosine kinase adaptor protein 1; qPCR, quantitative PCR; PBS, phosphate-buffered saline; Rac1, Ras-related C3 botulinum toxin substrate 1; ROC, receiver operating characteristic; SH, Src homology; si, small interfering; SPF, specific pathogen-free; WASP, Wiskott-Aldrich syndrome family protein.

***Correspondence to:** Xianzhang Huang, Department of Clinical Laboratory, Second Affiliated Hospital to Guangzhou University of Chinese Medicine, 58 Dade Road, Guangzhou, Guangdong 510120, China. ORCID: https://orcid.org/0000-0003-4320-9181. Tel: +86-13544549165, Fax: +86-20-81887233, E-mail: huangxz020@gzucm.edu.cn

poor cancer prognosis.[13]

In HCC, DCD has been reported as a factor affecting survival.[12] DCD levels were found to be significantly elevated in HCC tissues and the sera of patients, and serum DCD levels were associated with tumor metastasis and thus could potentially be a biomarker for HCC diagnosis.[23] Previous studies also revealed that noncatalytic region of tyrosine kinase adaptor protein 1 (Nck1), a Src homology (SH) 2 and SH3 domain-bearing protein, can bind to Wiskott-Aldrich syndrome protein (WASP) and modulate reorganization of the actin cytoskeleton and cell mobility.[24] The phosphotyrosine residue at position 20 of the DCD molecule was found to be crucial to its interaction with Nck1.[18] Moreover, actin cytoskeleton reorganization caused by different Rho GTPases (e.g., Ras-related C3 botulinum toxin substrate 1 [Rac1] and cell division control protein 42 homologue [Cdc42]) binds to WASP and activates the WASP/ actin-related protein 2/3 (Arp2/3) complex[25] for cell growth, migration, and adhesion.[26–29] In this context, fibronectin, a glycoprotein of the extracellular matrix,[30] also influences cell growth, adhesion, migration, and/or differentiation.[30] Dysregulated fibronectin expression was found to cause cancer and liver fibrosis.[31,32] Other publications showed that DCD can bind to the Nck1 SH2 domain and activate Rac1, Cdc42,[18] and ρ-GTPases[18] to promote HCC cell migration;[18] although, the signaling mechanisms that facilitate cell adhesion, growth and migration in HCC have not been thoroughly elucidated.

In this study, we assessed the effects of DCD overexpression and knockdown on the regulation of HCC cell phenotypes and the expression of Nck1, Rac1, Cdc42, WASP, and Arp2/3 *in vitro* and in nude mice.

Methods

Patients

The study protocol was approved by the Institutional Human Research Committee of Guangzhou Hospital of Traditional Chinese Medicine (Guangzhou, China), with approval number 2015NK001, and conducted following the standards set by the Declaration of Helsinki. Each patient provided written informed consent. The study cohort included 105 patients with HCC and 42 healthy controls (non-cirrhotic and non-HCC individuals).

The patients were treated at Guangzhou Hospital of Traditional Chinese Medicine between October 2016 and May 2017. There were 83 men and 22 women, with a median age of 56.37 years. The control individuals visited our hospital for an annual health check, and had no abnormal findings. The patients and healthy controls were demographically matched. The inclusion criteria were HCC diagnosed histologically according to the Standardization of Diagnosis and Treatment for Hepatocellular Carcinoma (2017 edition) without any pretreatment or other malignancies and aged 18 years or older.

Enzyme-linked immunosorbent assay (ELISA)

Blood samples were requisitioned from both the patients and controls for ELISA analysis of the serum DCD levels using a human DCD ELISA kit (Cat. #KT-13259; Kaniya Biomedical, Fullerton, CA, USA). According to the manufacturer, this ELISA was a double-antibody sandwich type with a high sensitivity and excellent specificity for DCD detection, with no significant cross-reactivity or interference between DCD and its analogue using the DCD antibody that recognizes *Homo sapiens* antigen. The procedures were conducted in accordance with the manufacturer's protocol. In brief, 100-μL serum samples were added to ELISA plates in triplicate and incubated at 37°C for 2 h. The solution was then rinsed out, and Buffer A from the kit was added for incubation at 37°C for 1 h. The wells were washed 3 times with 350 μL of the washing solution for 2 m, after which 100 μL of Buffer B was added and incubated at 37°C for 30 m. Thereafter, the wells were washed 5 times with the washing solution and 90 μL of the color solution was added; after incubation at 37°C for up to 25 m in the dark, stop solution was added and mixed well. Then, the solution was measured at 450 nm using a spectrophotometer (Fenghua, Guangzhou, China). The measurement was repeated at least once.

Cell line, culture, and transfection

HCC SK-HEP-1 cells were purchased from the cell bank of the Chinese Academy of Medical Sciences (Shanghai, China) and grown in high-glucose Dulbecco's modified Eagle's medium (DMEM; Gibco, Clayton, VIC, Australia) containing 10% fetal bovine serum (Gibco), 100 U/mL penicillin, and 100 μg/mL streptomycin in a humidified incubator containing 5% CO_2 at 37°C.

The *DCD* cDNA was PCR-amplified and subcloned into pReciever M06 (FulenGen, Guangzhou, China), while the GST-tagged SH2 domain of *Nck* cDNA was constructed using PCR amplification with a human *Nck* cDNA template and ligated into pGEX-4T-3 (GE Healthcare, Fairfield, CT, USA). After confirming the DNA sequencing, these vectors were transfected into SK-HEP-1 cells using Lipofectamine 2000 (Invitrogen, Carlsbad, CA, USA) in accordance with the manufacturer's protocol. *DCD* small interfering (si)RNA and negative control siRNA (NC) were obtained from FulenGen and transfected into the SK-HEP-1 cells using Lipofectamine 2000. The DCD siRNA targeting sequence was 5'-AGACGTCCTTGACTCAGTA-3', while the NC sequences were not disclosed by the manufacturer.

Immunofluorescent detection of NCK and DCD in SK-HEP-1 cells

DCD cDNA-, siRNA-, or NC-transfected SK-HEP-1 cells were subjected to immunofluorescence staining of DCD and NCK proteins using anti-DCD and NCK antibodies (Santa Cruz Biotechnology, Dallas, TX, USA), respectively. The procedures were conducted in accordance with the manufacturer's recommended protocol. Images were then captured with a fluorescence microscope (Olympus, Tokyo, Japan).

Western blot analysis

Western blotting was utilized to assess changed protein levels according to a previous study.[33] Primary antibodies against DCD, Nck1, and GAPDH were purchased from Abcam (Cambridge, MA, USA), Santa Cruz Biotechnology, and Sigma-Aldrich (St. Louis, MO, USA), respectively.

RT-quantitative (q)PCR

Total cellular RNA was isolated using TRIzol reagent (Invitrogen) in accordance with the manufacturer's instructions. cDNA was synthesized via reverse transcription with 1-μg RNA samples of each using a Geneseed II First Strand cDNA Synthesis Kit (Geneseed Biotech, San Diego, CA, USA).

qPCR was then used to amplify different genes using

Geneseed qPCR SYBR Green Master Mix in an ABI Prism 700 machine in accordance with the manufacturer's protocol. The primer sequences are listed in Supplementary Table 1. The PCR conditions were set to a hot start at 95°C for 5 m, followed by 40 cycles of 95°C for 10 s and 60°C for 34 s, and a melting program of 95°C for 15 s, 60°C for 60 s, and 95°C for 15 s. The relative level of mRNA was normalized to *GAPDH* mRNA and expressed as $2^{-\Delta\Delta Ct}$.

Transwell assay

SK-HEP-1 cells ($0.5–1.0\times10^5$ cells/well) were cultured in the upper chambers of 24-well Transwell plates with 8.0-μm pore filters (BD Biosciences, San Jose, CA, USA). The bottom chambers were filled with complete cell growth medium. The cells were treated in duplicate with vehicle alone, doxorubicin (Adriamycin; 5 μg/mL), or different concentrations (10–30%) of Mahong and cultured for 8 h. The difference between the migration and invasion assays was the filter used in the Transwells, i.e. precoated with 50 μL of Matrigel (BD Biosciences) for the invasion assay or not subjected to any pretreatment for the migration assay.

The cells on the surface of the upper chamber membrane were carefully removed using cotton swabs, and the migrated or invaded cells at the bottom surface of the upper chamber membrane were fixed and stained with 0.5% crystal violet in 70% ethanol and photographed under a light microscope (YS100; Nikon, Tokyo, Japan). The numbers of migrated or invaded cells in five fields of each upper chamber were counted in a blinded manner. For the invasion assay, the Transwell filters were precoated with Matrigel (BD Biosciences) for 24 h.

Rac1 and Cdc42 activation assay

The intracellular activity of the Rac1 and Cdc42 GTPases was measured with Rac1 and Cdc42 activation assay kits (Upstate Biotechnology, Lake Placid, NY, USA), respectively, and conducted in accordance with the manufacturer's instructions. In particular, cells were washed with ice-cold phosphate-buffered saline (PBS) and lysed with Mg^{2+} lysis/wash buffer. The samples were clarified using glutathione agarose and quantified, and equal aliquots of protein were incubated with the Rac/Cdc42 assay reagent (PAK-1PBD, agarose) at 4°C for 1 h. GTP-S-pretreated lysate was used as a positive control. GTP-bound Rac1 and Cdc42 were precipitated and eluted in Laemmli reducing sample buffer, resolved by 12% sodium dodecyl sulfate-polyacrylamide gel electrophoresis and blotted with monoclonal anti-Rac1 or Cdc42 antibody. The cell lysate (5%) was also subjected to Western blotting using these two monoclonal antibodies to assay the total amount of Rac1 and Cdc42.

SK-HEP2 cell orthotopic mouse model

The animal study protocol was approved by the ethics committee of Guangzhou Hospital of Traditional Chinese Medicine. This study was conducted in accordance with the Guidelines of the Care and Use of Laboratory Animals issued by the Chinese Council on Animal Research. Specifically, 20 male Balb/c nude mice, 6–7 weeks-old, were obtained from the Animal Experimental Center of Guangzhou Yuanshen Biomedical Technology (Guangzhou, China), quarantined in a specific pathogen-free (SPF) barrier facility, and housed under controlled temperature and humidity with alternating 12-h light and dark cycles. The mice received SPF mouse chow and were allowed to drink sterile water *ad libitum* for 7 days before the experiments.

For our experiments, SK-HEP2-luc and HEP2-luc-DCD cells (1×10^6 cells/injection), obtained by the stable transfection of *DCD* cDNA into SK-HEP-1 cells using lentivirus carrying pCDH-DCD-copGFP or pCDH-DCD-LUC-copGFP, were injected into mouse liver. The mice were anesthetized using 3% isoflurane and the abdomen opened to expose the liver for a direct injection of the tumor cells (2×10^7 cells/mL in 50 μL PBS) into the liver. The injection site was sealed with biogum, and the abdomen was then sutured. These mice had free access to food and water; water bottles were fitted with extended 3.5-inch spouts. Mice that were unable to walk were hand-watered. The mice were left to recover. The mice were monitored daily, and the data were recorded every 3 days. On day 26 after tumor cell transplantation, metastatic lesions within the liver and abdomen were examined under luciferin light (Abcam). At the end of the experiments, the mice were euthanized by intraperitoneal injection of 160 mg/kg sodium pentobarbital.

Statistical analysis

The data were expressed as the mean±standard deviation of three independent experiments. Statistical analyses of normally distributed continuous data were performed using the unpaired *t*-test. Comparisons of multiple groups of data with confidence intervals among and between groups were analyzed using one-way analysis of variance and then Bonferroni correction or Dunnett's tests, respectively. The diagnostic value of the serum DCD level in patients was assessed using a receiver operating characteristic (ROC) curve and logistic regression analyses by calculation of the area under the ROC curve (AUC). All statistical analyses were performed using Statistica 19.0 (Palo Alto, CA, USA). A p value <0.05 was considered statistically significant.

Results

Demographic and clinicopathological characteristics of patients

Our data showed no significant difference in the demographic data between the patient and control groups (Supplementary Table 2). However, the serum DCD levels were significantly higher in the patients than in the healthy controls. The ROC analysis showed that DCD could be used as a diagnostic marker of HCC (AUC=0.856, 95% confidence interval [CI]: 0.789–0.908). The optimum DCD cutoff value was 18.87 ng/mL, with sensitivity of 74.29% (95% CI: 64.8–82.3%) and specificity of 92.86% (95% CI: 80.5–98.5%); the positive predictive value and negative predictive value at this cutoff level were 96.3% (95% CI: 89.6–99.2%) and 59.1% (95% CI: 46.3–71.0%), respectively (Table 1, Fig. 1 and Supplementary Table 2).

Upregulated expression of DCD and Nck1 in HCC cells

DCD protein was able to bind to the Nck1-SH2 domain in HCC tissues. Their coexpression *in vitro* was verified using immunofluorescence microscopy. *DCD* overexpression plasmids or *DCD*-siRNA were transfected for 48 h into SK-HEP-1 cells, and the DCD and NCK levels were detected by immunofluorescence. Images were captured under an immunofluorescence microscope. The data showed that both DCD and NCK were localized in the cytoplasm and nuclei in the control cells and increased after *DCD* cDNA transfection.

Table 1. ROC analysis of the DCD value in HCC diagnosis

	Value	95% CI
AUC	0.856	0.789–0.908
DCD cutoff	18.87	–
Se	74.29	64.8–82.3
Sp	92.86	80.5–98.5
+LR	10.4	3.5–31.1
–LR	0.28	0.2–0.4
+PV	96.3	89.6–99.2
–PV	59.1	46.3–71.0

ROC, receiver operating characteristic; Se, sensitivity; Sp, specificity; +LR, positive likelihood ratio; –LR, negative likelihood ratio; +PV, positive predictive value; –PV, negative predictive value; Se, sensitivity; Sp, specificity.

However, *DCD*-siRNA transfection led to the expression of both DCD and NCK in the nuclei (although their levels were lower; Fig. 2).

Effects of DCD on the expression of Rac1, Cdc42, fibronectin, WASP, and Arp2/3 in SK-HEP-1 cells

DCD cDNA-transfected SK-HEP-1 cells showed a significant increase in the mRNA levels of *DCD*, *Arp2/3*, *WASP* and *fibronectin*, whereas transfection of *DCD*-siRNA significantly decreased the mRNA levels of these genes (Fig. 3A, E), while transfection of *DCD*-siRNA significantly increased the level of Arp2/3 (mRNA; Fig. 3C). Moreover, transfection of *DCD* cDNA also significantly induced the protein levels of DCD, active Rac1, active Cdc42, fibronectin, WASP, and Arp2/3, whereas transfection of DCD-siRNA significantly decreased the protein levels of DCD, active Rac1, active Cdc42, fibronectin, WASP, and Arp2/3 in HCC cells (Fig. 3F, G).

Effects of DCD manipulation on SK-HEP-1 cell migration and invasion

Transfection of *DCD* cDNA significantly increased tumor cell migration and invasion, whereas transfection of *DCD*-siRNA significantly decreased these cell numbers in SK-HEP-1 cells (Fig. 4A, B).

Rac1 attenuation of DCD-siRNA-mediated inhibition of SK-HEP-1 cell migration and invasion

Transfection of *Rac1* cDNA significantly increased HCC cell migration and invasion, and transfection of *Rac1* cDNA into HCC cells after *DCD*-siRNA transfection also attenuated the inhibitory effects of *DCD*-siRNA on SK-HEP-1 cell migration and invasion (Fig. 4C, D).

Rac1 rescued the expression of active Rac1/total Rac1, WASP, Arp2/3, and fibronectin in DCD-siRNA-transfected SK-HEP-1 cells

The levels of different proteins were assessed after transfection of Rac1 into SK-HEP-1 cells with previous *DCD*-siRNA transfection. The data showed a significant decrease in the levels of DCD, active Rac1/total Rac1, WASP, Arp2/3, and fibronectin proteins in *DCD*-siRNA-transfected SK-HEP-1 cells (Fig. 5). Transfection of *Rac1* cDNA in SK-HEP-1 cells significantly ($p<0.01$) increased the levels of active Rac1/total Rac1, WASP, Arp2/3 and fibronectin protein. However, cotransfection of *DCD*-siRNA and *Rac1* cDNA led to the levels of active Rac1/total Rac1, WASP, Arp2/3 and fibronectin proteins reaching those of the control in SK-HEP-1 cells.

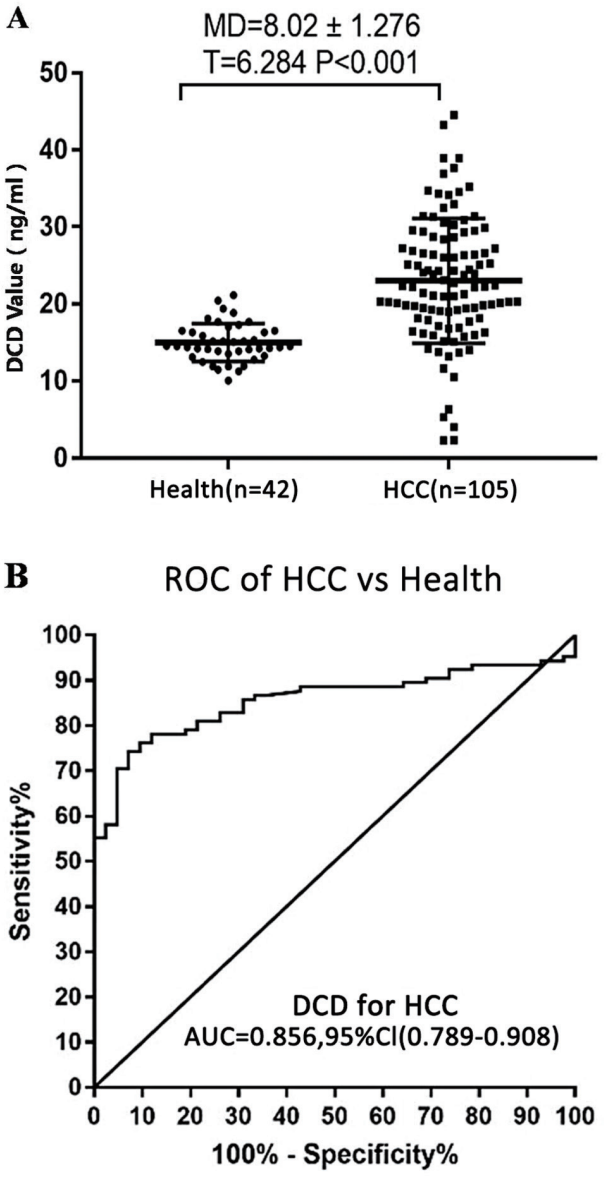

Fig. 1. Detection of serum DCD values as a diagnostic marker for HCC. (A) ELISA comparison of DCD levels between patients with HCC and healthy controls. (B) ROC analysis of the DCD levels in patients, showing that DCD diagnosis of HCC had an AUC of 0.856 (95% CI: 0.789–0.908). DCD, dermcidin; HCC, hepatocellular carcinoma; ELISA, enzyme-linked immunosorbent assay; ROC, receiver operating characteristic.

Effect of DCD on the regulation of SK-HEP-1 cell metastasis in mice

SK-HEP2-luc and HEP2-luc-DCD cells were injected into mouse liver, and on day 26 after transplantation, fluores-

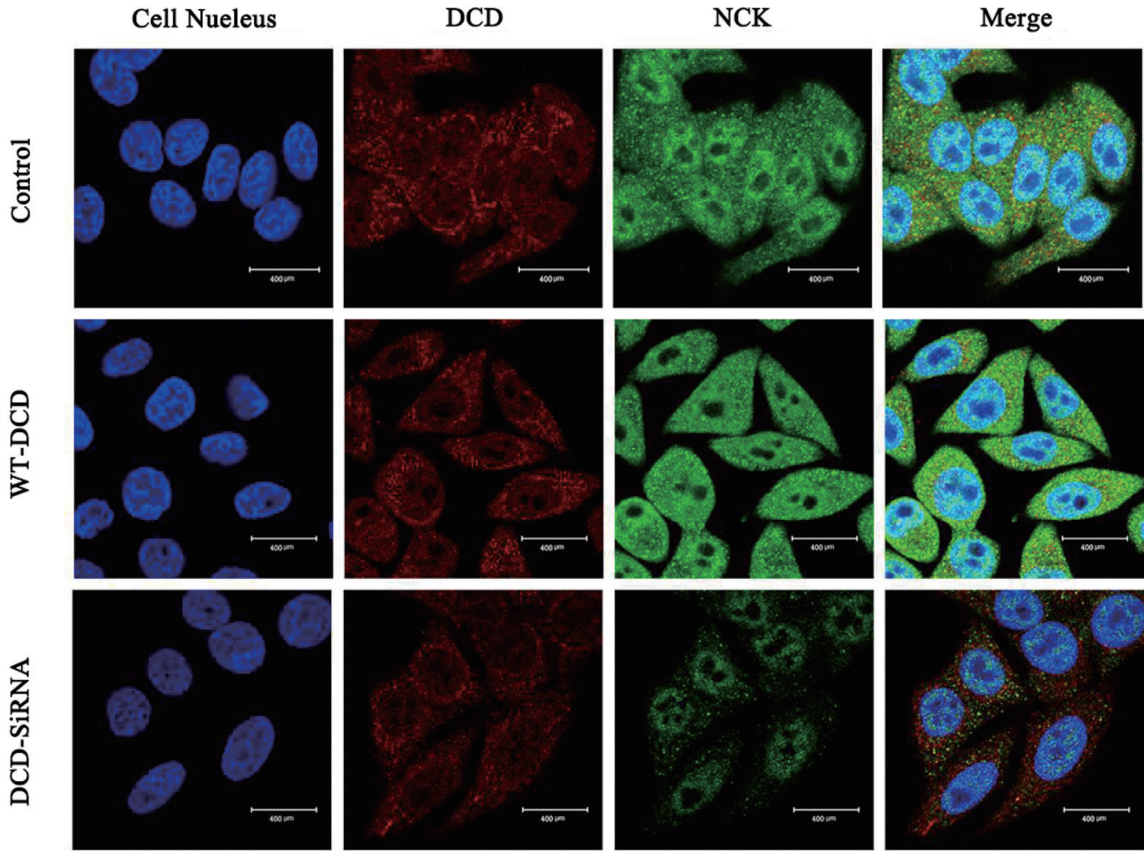

Fig. 2. Colocalization of DCD and NCK proteins in SK-HEP-1 cells. *DCD* overexpression plasmids were transfected into SK-HEP-1 cells, and 48 h after transfection, DCD and NCK were detected with fluorescence-labeled DCD antibody or NCK antibody, respectively. DCD was mainly detected in the cytoplasm, while NCK was mainly detected in both the cytoplasm and nuclei, and NCK colocalized with DCD in HCC cells. Magnification, 200×. The length of the scale bars is 400 μm. DCD, dermcidin; Nck, noncatalytic region of tyrosine kinase adaptor protein 1.

cence revealed that two-thirds of the mice implanted with HEP2-luc-DCD cells showed metastatic lesions in the liver and abdomen. SK-HEP2-luc cells only showed metastatic lesions within the liver but without abdominal lesions in the mice (Fig. 6).

Discussion

In the current study, we found that the DCD level was higher in the sera of patients with HCC and in SK-HEP-1 cells. The detection of serum DCD levels could be used as a diagnostic marker for HCC. Furthermore, both DCD overexpression and knockdown influenced the expression of *Nck1*, *Rac1*, *Cdc42*, *fibronectin*, *WASP*, and *Arp2/3*, the ability of HCC cells to migrate and invade *in vitro* and tumor cell metastasis in nude mice. These results showed that DCD-promoted HCC cell migration, invasion, and metastasis were affected through regulation of NCK and its downstream signaling pathway (Fig. 7).

Indeed, our current data on an increase in serum DCD levels are consistent with our previous study[23] and support the possibility of serum DCD levels being used as a biomarker for HCC diagnosis.[23] However, there was a different serum DCD cutoff value used between the current study and our previous study,[23] i.e. 18.87 ng/mL and 25.75 ng/mL, respectively. This may be due to the differences in sizes of the patient and control populations of the two studies. A future study with a larger sample size from multiple institutions is needed to verify the true cutoff for serum DCD in HCC diagnosis. Moreover, *DCD* overexpression led to increases in HCC cell migration and invasion, while knockdown of *DCD* expression reduced the capacity of SK-HEP-1 cell migration and invasion in culture, and DCD overexpression induced HCC cell abdominal metastasis *in vivo*. Similar data have been observed in other cancers[19–22] with further confirmation that DCD expression is associated with cancer progression and unfavorable prognosis.[13] Taken together, DCD has the potential to be used as a diagnostic and prognostic biomarker for HCC.

The colocalization of DCD and Nck1 proteins in SK-HEP-1 cell cytoplasm and nuclei was consistent with the data showing that DCD binds to the Nck1-SH2 domain in HCC after coimmunoprecipitation-Western blot analysis.[18] Nck1, as a SH2 and SH3 domain-bearing protein, can bind to WASP and modulate actin cytoskeleton reorganization through the WASP/Arp2/3 complex and promote cell directional migration via pseudopodia.[24] Indeed, the phosphorylated tyrosine residue at position 20 of the DCD molecule was crucial to its interaction with Nck1.[18] However, tyrosine residue 20 is not a part of the signaling peptides, the survival promoting peptide (Y-P30) or proteolysis inducing factor. It may not be possible to attribute the DCD function to interaction with Nck1; thus, further investigation using specific antibodies and genetic approaches is needed to better understand the underlying molecular mechanisms. Moreover, our observations showed that overexpression of *DCD* increased the expression of *Nck1* and cell migration and invasion, whereas knockdown of *DCD*

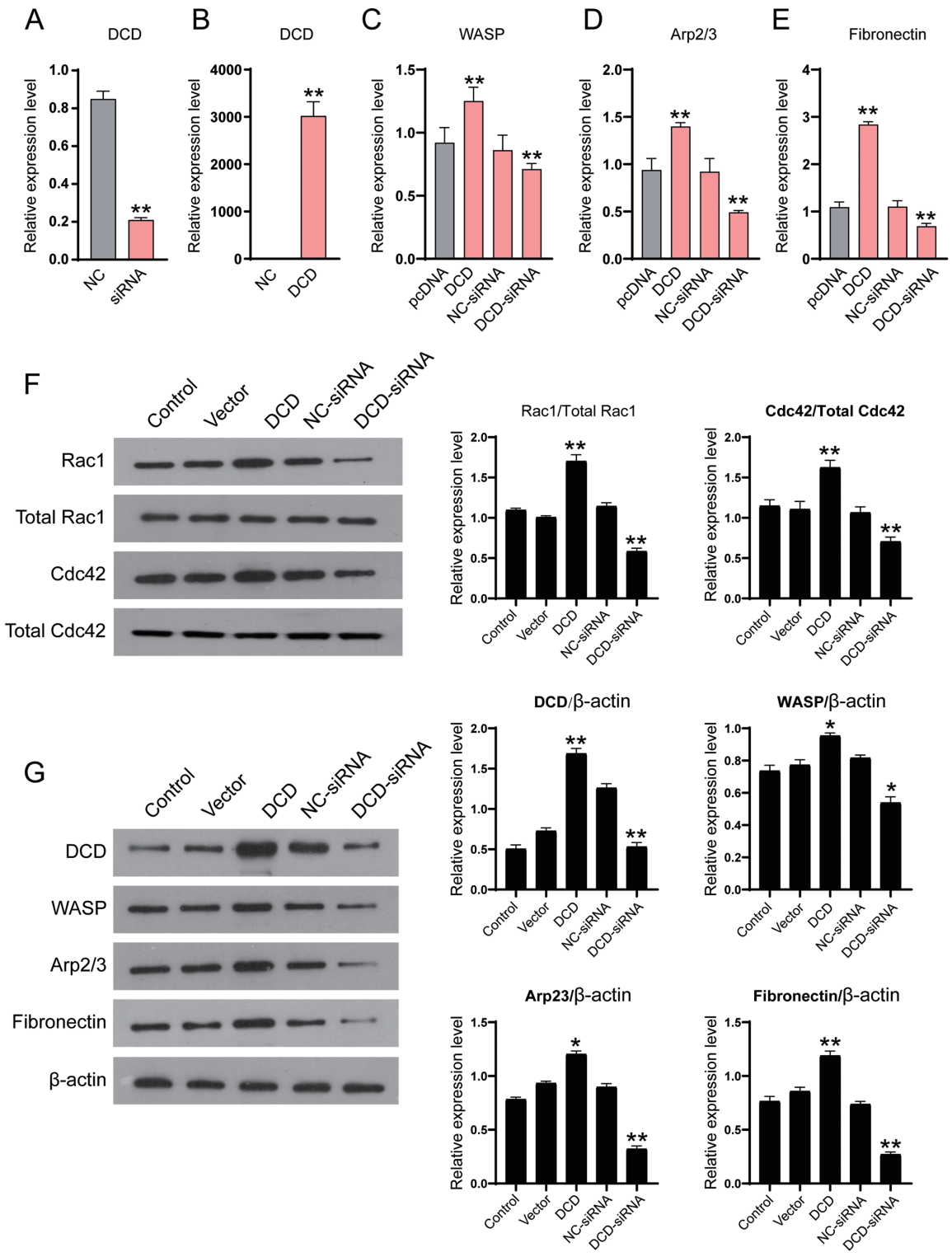

Fig. 3. Detection of the DCD, fibronectin, WASP, and Arp2/3 mRNA and protein levels in SK-HEP-1 cells. (A) Level of *DCD* mRNA in SK-HEP-1 cells after transfection with *DCD* siRNA. (B) Level of *DCD* mRNA in SK-HEP-1 cells after transfection with *DCD* cDNA. (C–E) Levels of *Arp2/3*, *WASP* and *fibronectin* mRNA in transfected SK-HEP1 cells. (F and G) SK-HEP-1 cells were transfected with an empty vector, wild-type *DCD* cDNA or *DCD* siRNA, and 48 h after transfection, the levels of DCD, active Rac1, active Cdc42, fibronectin, WASP, and Arp2/3 protein were determined by Western blotting. Comparisons of multiple groups of data with confidence intervals among and between groups were analyzed using one-way analysis of variance and then Bonferroni correction or Dunnett's tests, respectively. The data show the mean±standard deviation (n=3). **p<0.01. DCD, dermcidin; Arp2/3, actin-related protein 2/3; Cdc42, cell division control protein 42 homologue; Rac1, Ras-related C3 botulinum toxin substrate 1; WASP, Wiskott-Aldrich syndrome family protein.

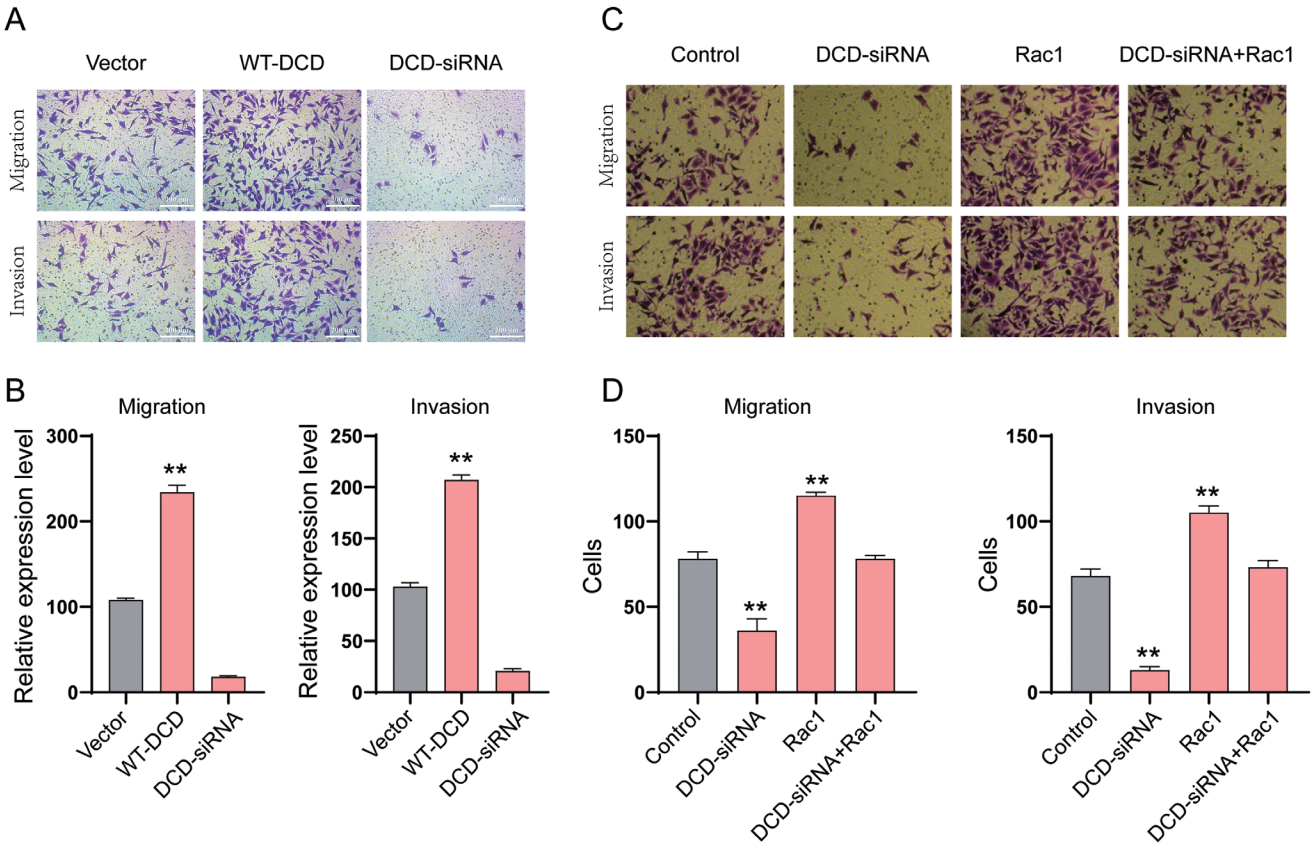

Fig. 4. Effects of DCD on HCC cell migration and invasion and attenuation of the *DCD*-siRNA-mediated suppression of SK-HEP1 cell migration and invasion. (A) Transfection was employed to introduce an empty vector, *DCD* expression vector, or *DCD* siRNA into SK-HEP-1 cells. Cells were then inoculated into the upper compartment of the chamber and cultured for 18 h. Cells and cell extensions that migrated through the pores of the Transwell plates (migration; magnification, 200×) and (B) cells that invaded Matrigel and their invasion extent were calculated. (C) SK-HEP-1 cells were transfected with *DCD*-siRNA, *Rac1* expression vector, or both for 48 h. (D) The rescuing effects of Rac1 on HCC cell migration and invasion of *DCD*-siRNA-transfected SK-HEP1 cells were detected. Photographs were taken under a phase-contrast Nikon microscope (magnification, 200×). Comparisons of multiple groups of data with confidence intervals among and between groups were analyzed using one-way analysis of variance and then Bonferroni correction or Dunnett's tests, respectively. The data show the mean±standard deviation (n=3). **p<0.01). The length of the scale bars is 200 μm. DCD, dermcidin; HCC, hepatocellular carcinoma; Rac1, Ras-related C3 botulinum toxin substrate 1.

expression decreased the expression of *Nck1*. Cell migration and invasion in cultured SK-HEP-1 cells revealed that Nck1 was involved in DCD-mediated HCC progression.

Reorganization of the actin cytoskeleton could be caused by different Rho GTPases, such as Rac1 and Cdc42, after binding to WASP and activation of the WASP/Arp2/3 complex.[25] Rac1, a Rho-like GTPase, modulates the cytoskeleton and influences cell growth, migration, and adhesion.[26–29] Rac1 is activated to induce the establishment of actin-rich lamellipodia protrusions at the leading edge of migrating cells and drives the cell membrane to extend for cell movement,[34,35] which leads to cell epithelial mesenchymal transition.[36,37]

Cdc42, a GTPase of the Rho family, modifies signaling pathways for diverse cellular functions, such as cell migration.[38] Activated Cdc42 binds to WASP, stimulates actin cytoskeleton remodeling, promotes the formation of filopodia[39–41] and pseudopodia,[42] and aids cell migration, invasion and metastasis.[42]

The WASP family comprises five members, including WASP and N-WASP, with a similar protein structure.[43] The Arp2/3 complex comprises seven-subunit proteins and plays a key role in regulation of the actin cytoskeleton.[44] WASP is activated after binding to Cdc42, PIP2,[43] and GTP-bound Rac1.[45,46] After activation, WASP can bind to the Arp2/3 complex.[47] The complex has affinity for the existing filaments and triggers elongation of a new filament as actin nucleation cores.[44] The formation of filopodia is required for cell motility[48] and promotes cell migration.[45,46]

In the current study, we also found that *DCD* overexpression increased the expression of WASP and Arp2/3, whereas knockdown of *DCD* expression decreased the expression of WASP and Arp2/3 in cultured SK-HEP-1 cells. Overexpression of *DCD* also increased the levels of active Rac1 and Cdc42 proteins, whereas transfection of *DCD*-siRNA decreased the levels of active Rac1 and Cdc42. All of these results indicate that DCD also regulates the activation of Rac1 and Cdc42 as well as the expression of WASP and Arp2/3, influences actin cytoskeleton modelling, and promotes cell migration, invasion, and metastasis in HCC (Fig. 7).[18,45,46] This was further confirmed by our observation that transfection of *Rac1* cDNA into *DCD*-siRNA-transfected SK-HEP-1 cells attenuated *DCD*-siRNA-induced suppression of HCC cell mobility and invasion and rescued the expression of active Rac1/total Rac1, WASP, and Arp2/3 proteins. Thus, overall, DCD protein binds to Nck through the Nck-SH2 domain to, in turn, activate WASP, leading to Rac1, Cdc42, and Arp2/3 activation and therefore to enhanced cell mobility. We also observed that DCD reduced the level of Arp2/3 mRNA but increased the level of Arp2/3 protein, indicating that DCD could regulate Arp2/3 at the transcriptional level but stabilized Arp2/3 protein; however, further study is needed to confirm and clarify this.

Fibronectin is a glycoprotein of the extracellular matrix[30]

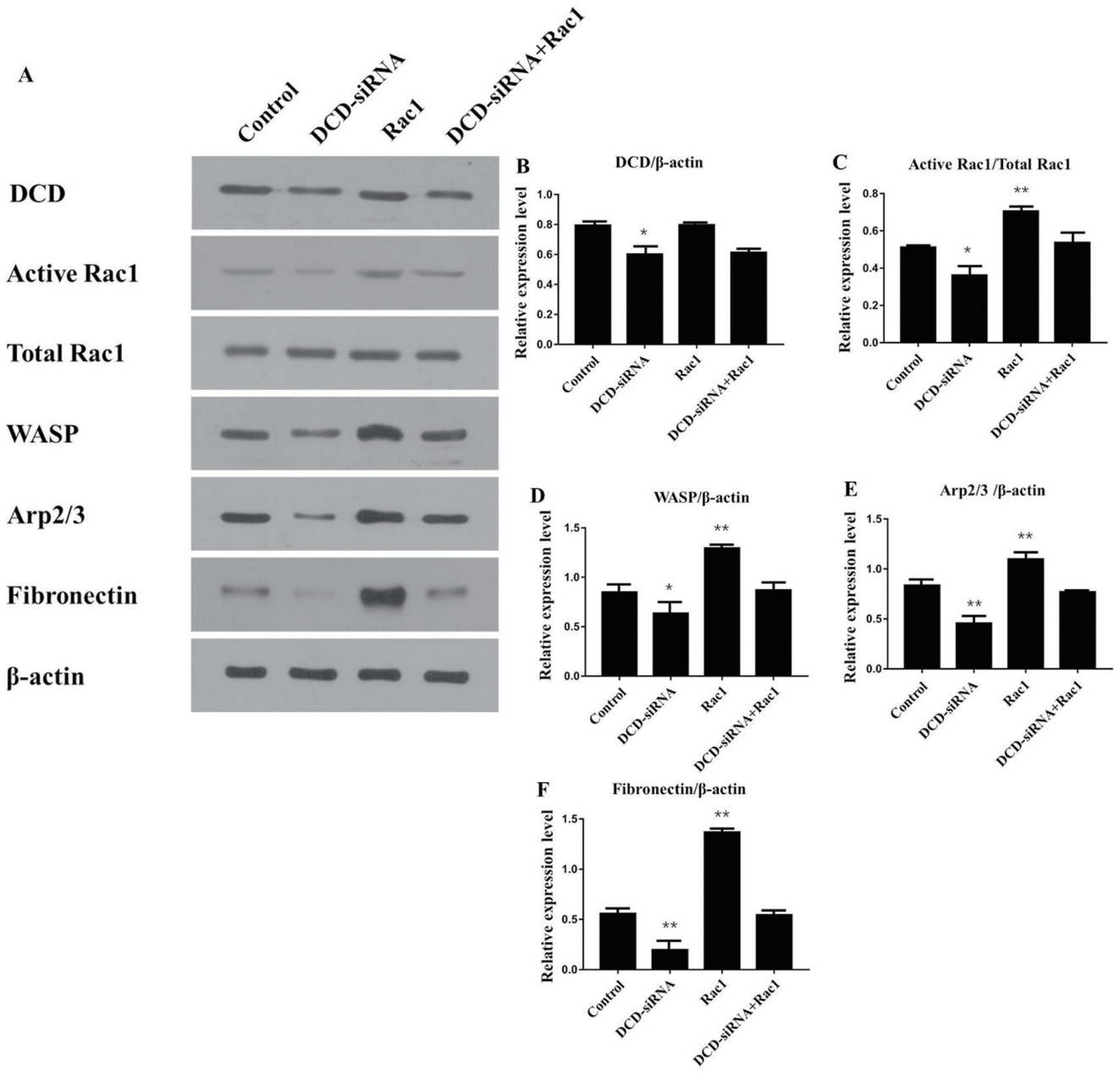

Fig. 5. *Rac1* rescue experiments of the active Rac1/total Rac1, WASP, Arp2/3, and fibronectin protein levels in *DCD*-siRNA-transfected SK-HEP-1 cells. SK-HEP-1 cells were transfected with *DCD*-siRNA, *Rac1* expression vector, or both and then subjected to Western blot analysis of active Rac1/total Rac1, WASP, Arp2/3, and fibronectin. (A) Western blotting. (B) DCD protein. (C) Active Rac1/total Rac1. (D) WASP protein. € Arp2/3 protein. (F) Fibronectin. Comparisons of multiple groups of data with confidence intervals among and between groups were analyzed using one-way analysis of variance and then Bonferroni correction or Dunnett's tests, respectively. The data show the mean±standard deviation (n=3). **p<0.01. Rac1, Ras-related C3 botulinum toxin substrate 1; WASP, Wiskott-Aldrich syndrome family protein; Arp2/3, actin-related protein 2/3; DCD, dermcidin.

that influences cell growth, adhesion, mobility, and differentiation.[30] Deregulated fibronectin expression causes cancer and fibrosis.[31,32] Overexpression of *DCD* increased the expression of fibronectin, while knockdown of *DCD* decreased the expression of fibronectin in cultured SK-HEP-1 cells. This suggests that DCD also promotes cell migration and invasion via fibronectin-mediated cell adhesion in HCC,[49] which was further demonstrated by *Rac1* rescue in *DCD*-siRNA-transfected SK-HEP-1 cells.

However, our current study does have some limitations. For example, the study is a proof-of-principle, and DCD's effects on HCC progression *in vivo* need further confirmation. Moreover, our nude mouse data only showed the effects of *DCD* cDNA *in vivo*, and there are no data on the inverse effects of *DCD* knockout *in vivo*. In conclusion, DCD protein levels were higher in the sera of patients with HCC and in SK-HEP-1 cells. DCD expression induced HCC cell migration, invasion, and metastasis *in vitro* and in nude mice by modulating Nck1, WASP, Arp2/3, and fibronectin expression and activating Rac1/Cdc42.

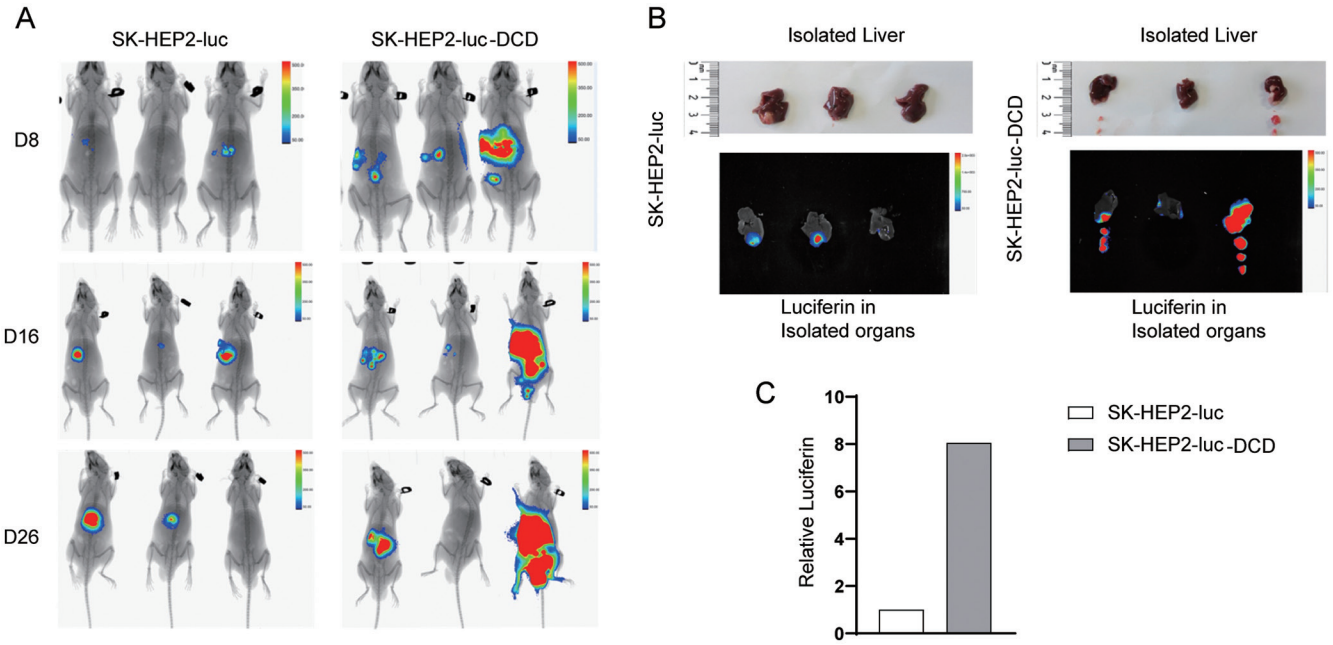

Fig. 6. Detection of HCC cell metastasis in SK-HEP-1 cell xenografts in mice. SK-HEP2-luc and HEP2-luc-DCD cells were injected into mouse liver, and on day 26 after transplantation, metastatic lesions were detected in the liver in mice implanted with HEP2-luc-DCD cells and abdominal metastatic lesions in 2/3 of mice implanted with HEP2-luc-DCD cells. There was only one tumor found in the primary implantation site but no metastatic lesions within the liver and abdomen. DCD, dermcidin.

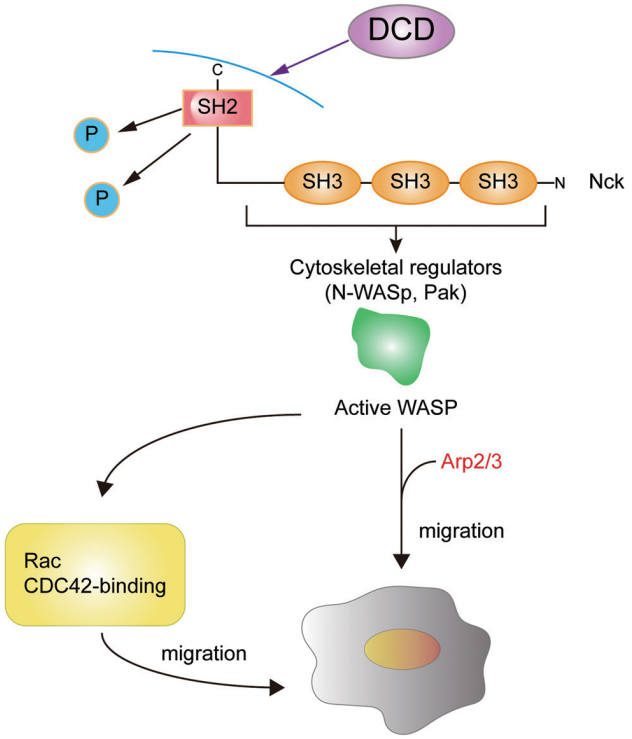

Fig. 7. Illustration of the DCD signaling network in the control of HCC cell migration. DCD binds to NCK to form the DCD/NCK/WASP/Arp2/3 complex, activates Rac1 and Cdc42 through cytoskeletal activity, and then modifies the cytoskeleton and induces HCC cell mobility. However, the data from this study showed that herb-inhibited DCD signaling could suppress HCC cell mobility. DCD, dermcidin; Nck, noncatalytic region of tyrosine kinase adaptor protein 1; WASP, Wiskott-Aldrich syndrome family protein; Arp2/3, actin-related protein 2/3; Cdc42, cell division control protein 42 homologue.

Funding

This study was supported in part by grants from Natural Science Foundation of Guangdong Province (#2021A1515010668), the National Natural Science Foundation of China (#81503424), the Guangzhou Science and Technology Innovation Commission (#201704020171), the Traditional Chinese Medicine Bureau of Guangdong Province (#20201263), and the Guangzhou Municipal Health and Health Committee (#20191A011014, #20202A011006, #20192A010005).

Conflict of interest

The authors have no conflict of interests related to this publication.

Author contributions

Study design (XH), Western blot experiments (FQ), *in vitro* studies (HL, LZ), biostatistical analyses (JL, ZY), and drafting of the manuscript (FQ, XH). All authors have read and approved the final version of this manuscript.

Data sharing statement

The data from the current study are available from the corresponding author upon reasonable request.

References

[1] Ghouri YA, Mian I, Rowe JH. Review of hepatocellular carcinoma: Epidemiology, etiology, and carcinogenesis. J Carcinog 2017;16:1. doi:10.4103/jcar.JCar_9_16, PMID:28694740.
[2] Chen C, Wang G. Mechanisms of hepatocellular carcinoma and chal-

lenges and opportunities for molecular targeted therapy. World J Hepatol 2015;7(15):1964–1970. doi:10.4254/wjh.v7.i15.1964, PMID:26244070.
[3] Ho DW, Lo RC, Chan LK, Ng IO. Molecular Pathogenesis of Hepatocellular Carcinoma. Liver Cancer 2016;5(4):290–302. doi:10.1159/000449340, PMID:27781201.
[4] Dhanasekaran R, Bandoh S, Roberts LR. Molecular pathogenesis of hepatocellular carcinoma and impact of therapeutic advances. F1000Res 2016;5(F1000 Faculty Rev):879. doi:10.12688/f1000research.6946.1, PMID: 27239288.
[5] Zhen C, Zhu C, Chen H, Xiong Y, Tan J, Chen D, *et al*. Systematic analysis of molecular mechanisms for HCC metastasis via text mining approach. Oncotarget 2017;8(8):13909–13916. doi:10.18632/oncotarget.14692, PMID:28108733.
[6] Schittek B. The multiple facets of dermcidin in cell survival and host defense. J Innate Immun 2012;4(4):349–360. doi:10.1159/000336844, PMID:22455996.
[7] Wang E, Qiang X, Li J, Zhu S, Wang P. The in Vitro Immune-Modulating Properties of a Sweat Gland-Derived Antimicrobial Peptide Dermcidin. Shock 2016;45(1):28–32. doi:10.1097/shk.0000000000000488, PMID:26529659.
[8] Burian M, Schittek B. The secrets of dermcidin action. IJMM 2015;305(2):283–286. doi:10.1016/j.ijmm.2014.12.012, PMID:25596890.
[9] Song C, de Groot BL, Sansom MSP. Lipid Bilayer Composition Influences the Activity of the Antimicrobial Peptide Dermcidin Channel. Biophys J 2019;116(9):1658–1666. doi:10.1016/j.bpj.2019.03.033, PMID:31010668.
[10] Muhlhauser P, Wadhwani P, Strandberg E, Burck J, Ulrich AS. Structure analysis of the membrane-bound dermcidin-derived peptide SSL-25 from human sweat. Biochim Biophys Acta Biomembr 2017;1859(12):2308–2318. doi:10.1016/j.bbamem.2017.09.004, PMID:28888369.
[11] Gerber MH, Underwood PW, Judge SM, Delitto D, Delitto AE, Nosacka RL, *et al*. Local and Systemic Cytokine Profiling for Pancreatic Ductal Adenocarcinoma to Study Cancer Cachexia in an Era of Precision Medicine. Int J Mol Sci 2018;19(12):3836. doi:10.3390/ijms19123836, PMID:30513792.
[12] Cottrill EE, Chen B, Adappa ND, Palmer JN, Kennedy DW, Lee RJ, *et al*. Expression of dermcidin in human sinonasal secretions. Int Forum Allergy Rhinol 2017;7(2):154–159. doi:10.1002/alr.21851, PMID:27650261.
[13] Bohlen J, McLaughlin SL, Hazard-Jenkins H, Infante AM, Montgomery C, Davis M, *et al*. Dysregulation of metabolic-associated pathways in muscle of breast cancer patients: preclinical evaluation of interleukin-15 targeting fatigue. J Cachexia Sarcopenia Muscle 2018;9(4):701–714. doi:10.1002/jcsm.12294, PMID:29582584.
[14] Molanouri Shamsi M, Chekachak S, Soudi S, Quinn LS, Ranjbar K, Chenari J, *et al*. Combined effect of aerobic interval training and selenium nanoparticles on expression of IL-15 and IL-10/TNF-alpha ratio in skeletal muscle of 4T1 breast cancer mice with cachexia. Cytokine 2017;90:100–108. doi:10.1016/j.cyto.2016.11.005, PMID:27863332.
[15] Rucci N, Capulli M, Olstad OK, Onnerfjord P, Tillgren V, Gautvik KM, *et al*. The alpha2beta1 binding domain of chondroadherin inhibits breast cancer-induced bone metastases and impairs primary tumour growth: a preclinical study. Cancer Lett 2015;358(1):67–75. doi:10.1016/j.canlet.2014.12.032, PMID:25529009.
[16] Stocki P, Wang XN, Morris NJ, Dickinson AM. HSP70 natively and specifically associates with an N-terminal dermcidin-derived peptide that contains an HLA-A*03 antigenic epitope. J Biol Chem 2011;286(14):12803–12811. doi:10.1074/jbc.M110.179630, PMID:21216960.
[17] Pathak S, De Souza GA, Salte T, Wiker HG, Asjo B. HIV induces both a down-regulation of IRAK-4 that impairs TLR signalling and an up-regulation of the antibiotic peptide dermcidin in monocytic cells. Scand J Immunol 2009;70(3):264–276. doi:10.1111/j.1365-3083.2009.02299.x, PMID: 19703016.
[18] Shen SL, Qiu FH, Dayarathna TK, Wu J, Kuang M, Li SS, *et al*. Identification of Dermcidin as a novel binding protein of Nck1 and characterization of its role in promoting cell migration. Biochim Biophys Acta 2011;1812(6):703–710. doi:10.1016/j.bbadis.2011.03.004, PMID:21397687.
[19] Zeth K, Sancho-Vaello E. The Human Antimicrobial Peptides Dermcidin and LL-37 Show Novel Distinct Pathways in Membrane Interactions. Front Chem 2017;5:86. doi:10.3389/fchem.2017.00086, PMID:29164103.
[20] Bancovik J, Moreira DF, Carrasco D, Yao J, Porter D, Moura R, *et al*. Dermcidin exerts its oncogenic effects in breast cancer via modulation of ERBB signaling. BMC cancer 2015;15:70. doi:10.1186/s12885-015-1022-6, PMID:25879571.
[21] Ustebay S, Baykus Y, Deniz R, Ugur K, Yavuzkir S, Yardim M, *et al*. Chemerin and Dermcidin in Human Milk and Their Alteration in Gestational Diabetes. J Hum Lact 2019;35(3):550–558. doi:10.1177/0890334419837523, PMID:31002762.
[22] Dash-Wagh S, Neumann JR, Veitinger S, Grote-Westrick C, Landgraf P, Pape HC, *et al*. The survival promoting peptide Y-P30 promotes cellular migration. Mol Cell Neurosci 2011;48(3):195–204. doi:10.1016/j.mcn.2011.07.005, PMID:21820515.
[23] Qiu F, Qiu F, Liu L, Liu J, Xu J, Huang X. The Role of Dermcidin in the Diagnosis and Staging of Hepatocellular Carcinoma. Genet Test Mol Biomarkers 2018;22(4):218–223. doi:10.1089/gtmb.2017.0230, PMID:29641283.
[24] Buvall L, Rashmi P, Lopez-Rivera E, Andreeva S, Weins A, Wallentin H, *et al*. Proteasomal degradation of Nck1 but not Nck2 regulates RhoA activation and actin dynamics. Nat Commun 2013;4:2863. doi:10.1038/ncomms3863, PMID:24287595.
[25] Chaki SP, Rivera GM. Integration of signaling and cytoskeletal remodeling by Nck in directional cell migration. Bioarchitecture 2013;3(3):57–63. doi:10.4161/bioa.25744, PMID:23887203.
[26] Herve JC, Bourmeyster N. Rho GTPases at the crossroad of signaling networks in mammals. Small GTPases 2015;6(2):43–48. doi:10.1080/21541248.2015.1044811, PMID:26110743.
[27] Hong J, Kim Y, Yanpallewar S, Lin PC. The Rho/Rac Guanine Nucleotide Exchange Factor Vav1 Regulates Hif-1alpha and Glut-1 Expression and Glucose Uptake in the Brain. Int J Mol Sci 2020;21(4):1341. doi:10.3390/ijms21041341, PMID:32079227.
[28] Yang W, Trahan GD, Howell ED, Speck NA, Jones KL, Gillen AE, *et al*. Enhancing Hematopoiesis from Murine Embryonic Stem Cells through MLL1-Induced Activation of a Rac/Rho/Integrin Signaling Axis. Stem Cell Reports 2020;14(2):285–299. doi:10.1016/j.stemcr.2019.12.009, PMID: 31951812.
[29] Xiang RF, Stack D, Huston SM, Li SS, Ogbomo H, Kyei SK, *et al*. Ras-related C3 Botulinum Toxin Substrate (Rac) and Src Family Kinases (SFK) Are Proximal and Essential for Phosphatidylinositol 3-Kinase (PI3K) Activation in Natural Killer (NK) Cell-mediated Direct Cytotoxicity against Cryptococcus neoformans. Stem Cell Reports 2016;291(13):6912–6922. doi:10.1074/jbc.M115.681544, PMID:26867574.
[30] Ao Q, Wang S, He Q, Ten H, Oyama K, Ito A, *et al*. Fibrin Glue/Fibronectin/Heparin-Based Delivery System of BMP2 Induces Osteogenesis in MC3T3-E1 Cells and Bone Formation in Rat Calvarial Critical-Sized Defects. ACS Appl Mater Interfaces 2020;12(11):13400–13410. doi:10.1021/acsami.0c01371, PMID:32091872.
[31] Gong Z, Chen M, Ren Q, Yue X, Dai Z. Fibronectin-targeted dual-acting micelles for combination therapy of metastatic breast cancer. Signal Transduct Target Ther 2020;5(1):12. doi:10.1038/s41392-019-0104-3, PMID: 32296050.
[32] Casanova MR, Reis RL, Martins A, Neves NM. Fibronectin Bound to a Fibrous Substrate has Chondrogenic-inductive Properties. Biomacromolecules 2020;21(4):1368–1378. doi:10.1021/acs.biomac.9b01546, PMID: 32003989.
[33] Stewart GD, Skipworth RJ, Pennington CJ, Lowrie AG, Deans DA, Edwards DR, *et al*. Variation in dermcidin expression in a range of primary human tumours and in hypoxic/oxidatively stressed human cell lines. Br J Cancer 2008;99(1):126–132. doi:10.1038/sj.bjc.6604458, PMID:18594538.
[34] Stankiewicz TR, Pena C, Bouchard RJ, Linseman DA. Dysregulation of Rac or Rho elicits death of motor neurons and activation of these GTPases is altered in the G93A mutant hSOD1 mouse model of amyotrophic lateral sclerosis. Neurobiol Dis 2020;136:104743. doi:10.1016/j.nbd.2020.104743, PMID:31931138.
[35] Parri M, Chiarugi P. Rac and Rho GTPases in cancer cell motility control. Cell Commun Signal 2010;8:23. doi:10.1186/1478-811X-8-23, PMID: 20822528.
[36] Stallings-Mann ML, Waldmann J, Zhang Y, Miller E, Gauthier ML, Visscher DW, *et al*. Matrix metalloproteinase induction of Rac1b, a key effector of lung cancer progression. Sci Transl Med 2012;4(142):142ra95. doi:10.1126/scitranslmed.3004062, PMID:22786680.
[37] Yang WH, Lan HY, Huang CH, Tai SK, Tzeng CH, Kao SY, *et al*. RAC1 activation mediates Twist1-induced cancer cell migration. Nat Cell Biol 2012;14(4):366–374. doi:10.1038/ncb2455, PMID:22407364.
[38] Qadir MI, Parveen A, Ali M. Cdc42: Role in Cancer Management. Chem Biol Drug Des 2015;86(4):432–439. doi:10.1111/cbdd.12556, PMID:25777055.
[39] Koike S, Yamasaki K, Yamauchi T, Shimada-Omori R, Tsuchiyama K, Ando H, *et al*. TLR3 stimulation induces melanosome endo/phagocytosis through RHOA and CDC42 in human epidermal keratinocyte. J Dermatol Sci 2019;96(3):168–177. doi:10.1016/j.jdermsci.2019.11.005, PMID:31776046.
[40] Liu C, Zhang L, Cui W, Du J, Li Z, Pang Y, *et al*. Epigenetically upregulated GEFT-derived invasion and metastasis of rhabdomyosarcoma via epithelial mesenchymal transition promoted by the Rac1/Cdc42-PAK signalling pathway. EBioMedicine 2019;50:122–134. doi:10.1016/j.ebiom.2019.10.060, PMID:31761617.
[41] Su W, Cheng CY. Cdc42 is involved in NC1 peptide-regulated BTB dynamics through actin and microtubule cytoskeletal reorganization. FASEB J 2019;33(12):14461–14478. doi:10.1096/fj.201900991R, PMID:31682474.
[42] Ye H, Zhang Y, Geng L, Li Z. Cdc42 expression in cervical cancer and its effects on cervical tumor invasion and migration. Int J Oncol 2015;46(2):757–763. doi:10.3892/ijo.2014.2748, PMID:25394485.
[43] Prehoda KE, Scott JA, Mullins RD, Lim WA. Integration of multiple signals through cooperative regulation of the N-WASP-Arp2/3 complex. Science 2000;290(5492):801–806. PMID:11052943.
[44] Veltman DM, Insall RH. WASP family proteins: their evolution and its physiological implications. Mol Biol Cell 2010;21(16):2880–2893. doi:10.1091/mbc.E10-04-0372, PMID:20573979.
[45] Zhao K, Wang D, Zhao X, Wang C, Gao Y, Liu K, *et al*. WDR63 inhibits Arp2/3-dependent actin polymerization and mediates the function of p53 in suppressing metastasis. EMBO Rep 2020;21:e49269. doi:10.15252/embr.201949269, PMID:32128961.
[46] Ridley AJ. Rho GTPase signalling in cell migration. Curr Opin Cell Biol 2015;36:103–112. doi:10.1016/j.ceb.2015.08.005, PMID:26363959.
[47] Ma W, Chang J, Tong J, Ho U, Yau B, Kebede MA, *et al*. Arp2/3 nucleates F-actin coating of fusing insulin granules in pancreatic beta cells to control insulin secretion. J Cell Sci 2020;133(6):jcs236794. doi:10.1242/jcs.236794, PMID:32079655.
[48] Tessier S, Doolittle AC, Sao K, Rotty JD, Bear JE, Ulici V, *et al*. Arp2/3 inactivation causes intervertebral disc and cartilage degeneration with dysregulated TonEBP-mediated osmoadaptation. JCI Insight 2020;5(4):e131382. doi:10.1172/jci.insight.131382, PMID:31961823.
[49] Hsiao CT, Cheng HW, Huang CM, Li HR, Ou MH, Huang JR, *et al*. Fibronectin in cell adhesion and migration via N-glycosylation. Oncotarget 2017;8(41):70653–70668. doi:10.18632/oncotarget.19969, PMID:29050309.